Contents lists available at ScienceDirect

J. Chem. Thermodynamics

Phase diagrams and thermodynamic modeling of solid-liquid equilibria in the system NaCl–KCl–SrCl$_2$–H$_2$O and its application in industry

Dan Li [a,*], Yuanhui Liu [b,*], Lingzong Meng [a,b,*], Yafei Guo [b], Tianlong Deng [b], Lan Yang [a]

[a] School of Chemistry and Chemical Engineering, Linyi University, Linyi 276000, China
[b] Tianjin Key Laboratory of Marine Resources and Chemistry, College of Chemical Engineering and Materials Science, Tianjin University of Science and Technology, Tianjin 300457, China

ARTICLE INFO

ABSTRACT

Combining of the determined solubilities of two ternary systems NaCl–SrCl$_2$–H$_2$O and KCl–SrCl$_2$–H$_2$O and Pitzer binary parameters obtained in the literature at different temperatures, the lacking Pitzer mixing parameters $\theta_{Na,Sr}$, $\theta_{K,Sr}$, $\Psi_{Na,Sr,Cl}$, and $\Psi_{K,Sr,Cl}$ were fitted on the basis of the Pitzer model. The variable temperature chemical model for Pitzer mixing parameters including Sr^{2+} ion was built. The model was then used to calculate thermodynamic properties such as the solubilities, osmotic coefficients, ionic activity coefficients and dilution enthalpy of the quaternary system NaCl–KCl–SrCl$_2$–H$_2$O in the wider temperature range. The theoretical results using the model coincide with the experimental values. The phase diagrams and Pitzer model for the quaternary system were then used to conduct computer simulation of isothermal evaporation and brine separation. The evaporation-crystallization route and the order of salt crystallization were obtained using the model at 298.15 K. The pure salts KCl, NaCl and SrCl$_2$·6H$_2$O were separated from the solution with the model at 273.15 K and 323.15 K.

© 2019 Elsevier Ltd.

1. Introduction

There are abundant potassium and strontium resources in oil-field brines and underground brines. The potassium concentration in oilfield brines of the Qinghai -Tibet Plateau can reach 35.75 g·L^{-1}, and the strontium concentration can reach 4.45 g·L^{-1}, which shows that the brines are valuable to exploit [1]. The system Li$^+$, Na$^+$, K$^+$, Ca^{2+}, Sr^{2+}//Cl$^-$, borate–H$_2$O can largely represent the brines. The comprehensive exploitation of brine resources has gradually been a research hotspot recently. Phase equilibria of salt–water systems can be used to guide the exploitation of brine resources [2,3]. Thermodynamic models are usually used to describe the phase equilibria for brine systems. The calculation of phase equilibrium solubilities of multi-component salt-water systems is of great importance in the fields of chemistry, chemical engineering and especially in the field of saline chemistry, such as the prediction of the evaporative path and the separation of minerals from brines by solar pond techniques. Among the numerous theories of the electrolyte solution, Pitzer theory characterizing

thermodynamics properties of electrolyte solution in brief and terse form is widely used either in geochemical behaviours of natural waters and mineral deposits or in the predictions of solubility of salt-water systems. The combination of the Pitzer electrolyte solution theory and the Harvie–Weare (HW) equations is called the Pitzer model [4–10].

Lithium salts are hard to saturate in brine, so the NaCl–KCl–SrCl$_2$–H$_2$O system can represent oilfield brine after multistep removal of calcium and boron. The experimental phase equilibria solubilities of the quaternary system NaCl–KCl–SrCl$_2$–H$_2$O and its ternary subsystems NaCl–SrCl$_2$–H$_2$O and KCl–SrCl$_2$–H$_2$O have been determined from 288.15 to 373.15 K [11–18]. The activity coefficients of KCl in the system KCl–SrCl$_2$–H$_2$O were determined by e. m.f. measurements, and Pitzer binary and ternary interaction parameters $\theta_{K, Sr}$ and $\Psi_{K, Sr, Cl}$ were evaluated at 298.15 K, 308.15 K and 318.15 K [19]. The mean activity coefficients for NaCl in the NaCl–SrCl$_2$–H$_2$O ternary system were determined by electrode potential measurements, and the Pitzer ion interaction parameters $\theta_{Na, Sr}$ and $\Psi_{Na, Sr, Cl}$ were obtained at 298.15 K [20]. The isopiestic measurements of the osmotic and activity coefficients of the NaCl–SrCl$_2$–H$_2$O ternary system at 298.15 K were made and an extended ion-interaction model was represented [21]. However, the thermodynamic model of these systems in the wider temperature range was not constructed because of the lack of the corresponding Pitzer mixing parameters including Sr^{2+} such

* Corresponding authors at: School of Chemistry and Chemical Engineering, Linyi University, Linyi 276000, China (D. Li and L. Meng); Tianjin University of Science and Technology, Tianjin 300457, China (Y. Liu).

E-mail addresses: lidan@lyu.edu.cn (D. Li), yhliu_suc@126.com (Y. Liu), menglingzong@lyu.edu.cn (L. Meng).

as $\theta_{Na,Sr}$, $\theta_{K,Sr}$, $\Psi_{Na,Sr,Cl}$, and $\Psi_{K,Sr,Cl}$. In this study, the variable temperature chemical model for Pitzer mixing ion interaction parameters including Sr^{2+} and the calculations of thermodynamic properties with the Pitzer model for the quaternary system $NaCl–KCl–SrCl_2–H_2O$ are presented from 273.15 K to 373.15 K. The phase diagrams and Pitzer model for the quaternary system were then used to conduct computer simulation of isothermal evaporation and brine separation.

2. Pitzer model

Pitzer thermodynamic model was widely used to calculate solubility, osmotic coefficient ø, ionic activity coefficients γ and dilution enthalpy et al. These main equations for thermodynamic property calculation are as follows [4–10].

$$(\phi - 1) = \left(2/\sum_i m_i\right)\left[-AI^{3/2}/\left(1 + bI^{1/2}\right)\right.$$
$$+ \sum_C \sum_a m_c m_a (B_{ca} + ZC_{ca})$$
$$+ \sum_c \sum_{<c'} m_c m_{c'}\left(\Phi_{cc'} + \sum_a m_a \Psi_{cc'a}\right)$$
$$\left. + \sum_a \sum_{<a'} m_a m_{a'}\left(\Phi_{aa'} + \sum_c m_c \Psi_{caa'}\right)\right] \tag{1}$$

$$ln\gamma_M = z_M^2 F + \sum_a m_a(2B_{Ma} + ZC_{Ma})$$
$$+ \sum_c m_c\left(2\Phi_{Mc} + \sum_a m_a\Psi_{Mca}\right) + \sum_a \sum_{<a'} m_a m_{a'}\Psi_{Maa'}$$
$$+ z_M \sum_c \sum_a m_c m_a C_{ca} \tag{2}$$

$$ln\gamma_X = z_X^2 F + \sum_c m_c(2B_{cX} + ZC_{cX})$$
$$+ \sum_a m_a\left(2\Phi_{Xa} + \sum_c m_c\Psi_{cXa}\right) + \sum_c \sum_{<c'} m_c m_{c'}\Psi_{cc'X}$$
$$+ |z_X| \sum_c \sum_a m_c m_a C_{ca} \tag{3}$$

$$ln a_w = -M_W \sum mi \tag{4}$$

In the above equations, $A^ø$ represents Debye–Hückel parameter. The subscripts M, c, c' and X, a, a' express the different cations and anions respectively. The symbols of m_c and Z_c are the mass molality and the charge of cation c. The other terms of F, C, Z, B and Φ in the above equations are defined in references [4–10]. In Eq. (4), a_w and M_w represent the water activity and molar mass of water $(kg \cdot mol^{-1})$, and the sum contains all solute species.

In the Pitzer model, $\beta^{(0)}$, $\beta^{(1)}$, $\beta^{(2)}$, $C^ø$ are Pitzer interaction parameters of single salts. $\theta_{cc'}$ and $\psi_{cc'a}$ represent Pitzer interaction parameters of mix ions: $\theta_{cc'}$ for each cation-cation and anion-anion pair; $\psi_{cc'a}$ for each cation-cation-anion and anion-anion-cation triplet. With the Pitzer model, the thermodynamic properties such as solubilities, water activities and so on can be calculated with the Pitzer parameters.

3. Model parameterization

The variable temperature chemical models for Pitzer single-salt parameters of NaCl and KCl, Pitzer mixing ion parameters $\theta_{Na, K}$ and $\Psi_{Na,K,Cl}$, and solubility products lnK_{sp} of NaCl and KCl were obtained with Eq. (5) from the literature [22]. The Pitzer single-

salt parameters of SrCl_2 and lnK_{sp} of strontium chloride salts can be calculated with the temperature-dependent Eq. (6) presented in the literature [23].

$$P(T) = a_1 + a_2 T + a_3/T + a_4 lnT + a_5/(T-263) + a_6 T^2$$
$$+ a_7/(680-T) + a_8/(T-227) \tag{5}$$

$$P(T) = a_1 + a_2(1/T - 1/T_R) + a_3 ln(T/T_R) + a_4(T-T_R)$$
$$+ a_5\left(T^2 - T_R^2\right) \tag{6}$$

where P is the parameters, T_R in Eq. (6) is 298.15 K.

On the basis of the Pitzer thermodynamic model and variable temperature chemical models for Pitzer single-salt parameters of NaCl, KCl and SrCl_2, Pitzer mixing ion parameters $\theta_{Na,Sr}$, $\theta_{K,Sr}$, $\Psi_{Na,Sr,Cl}$, and $\Psi_{K,Sr,Cl}$ were fitted with experimental solubility data of ternary systems $NaCl–SrCl_2–H_2O$ and $KCl–SrCl_2–H_2O$ at different temperatures in the wider temperature range (273.15 ~ 373.15 K). Then the temperature dependence of the interaction parameters including Sr^{2+} with Eq. (5) is obtained, whose constants are illustrated in Table 1.

4. Thermodynamic property calculation

4.1. Solubility calculation

Through solving the nonlinear coupled equations on equilibrium relation between solid and liquid phases with quasi-newton method and dichotomy method, the phase equilibrium solubilities in the quaternary system $NaCl–KCl–SrCl_2–H_2O$ and its ternary subsystems $NaCl–SrCl_2–H_2O$ and $KCl–SrCl_2–H_2O$ from 273.15 K to 373.15 K were achieved with the Pitzer parameters and lnK_{sp} values for the corresponding solid salts.

The calculated phase diagrams are shown in Figs. 1–3. Part of the predictive solubility data of the quaternary system $NaCl–KCl–SrCl_2–H_2O$ at 273.15 K are listed in Table 2 because the phase equilibrium solubilities have not been measured in literatures at 273.15 K. The results in Figs. 1 and 2 show that equilibrium curves corresponding to solid and liquid phases gradually ascend along with rising temperature in two ternary systems $NaCl–SrCl_2–H_2O$ and $KCl–SrCl_2–H_2O$. In the phase diagram of system $NaCl–KCl–SrCl_2–H_2O$ in Fig. 3, the Jänecke indices (J) for NaCl, KCl, SrCl_2 were calculated with the unit g/100 g dry salt ($m_{NaCl} + m_{KCl} + m_{SrCl2}$). In Fig. 3, the crystallization fields for $SrCl_2 \cdot 6H_2O$ and KCl obviously narrow, while the field for NaCl clearly broadens with increasing temperature. The comparison between calculated and experimental phase equilibrium solubilities were illustrated in Figs. 1(b), 2 (b), and 3(b). It is clear that calculated values are in excellent agreement with experimental equilibrium solubilities. The better agreement exhibits that Pitzer mixing ion parameters containing Sr^{2+} in this work are reliable from the temperature-dependent equations. The variable temperature model can be used to predict the solubility of complex brine and make up the lack of experimental solubility data in broader temperature ranges.

4.2. Osmotic coefficients, water activity and ionic activity coefficients calculation

Using the variable temperature chemical model in this work and literatures [22,23], the osmotic coefficients, water activity and ionic activity coefficients of equilibrium liquid of the quaternary system $NaCl–KCl–SrCl_2–H_2O$ were calculated. The results at 273.15 K are also shown in Table 2. These thermodynamic properties regularly change as shown in Table 2. The calculated water activity and activity coefficients for Sr^{2+} were plotted in Figs. 4 and 5. It illustrates that water activity has minimum value at

Table 1
The constants in the temperature equation (5) for mix parameters in the quaternary system NaCl–KCl–SrCl$_2$–H$_2$O.

Species	a_1	a_2	a_3	a_4	Ref.
$\theta_{Na,K}$	−5.02312111E−02	0	1.40213141E+01	0	[22]
$\Psi_{Na,K,Cl}$	1.34211308E−02	0	−5.10212917E+00	0	[22]
$\theta_{Na,Sr}$ (273.15–333.00 K)	3.13375454E+01	0	−1.73458255E+03	−4.46958066E+00	This work
$\theta_{Na,Sr}$ (333.15–373.15 K)	1.49215672E−01	0	0	0	This work
$\Psi_{Na,Sr,Cl}$ (273.15–333.00 K)	−7.49288202E+00	0	4.11575434E+02	1.07320263E+00	This work
$\Psi_{Na,Sr,Cl}$ (333.15–373.15 K)	−1.74340806E−02	0	0	0	This work
$\theta_{K,Sr}$ (273.15–298.15 K)	−4.23638479E−01	1.53327970E−03	0	0	This work
$\theta_{K,Sr}$ (298.15–323.15 K)	4.10729220E−01	−1.00398346E−03	0	0	This work
$\theta_{K,Sr}$ (323.25–373.15 K)	1.11918891E+00	−3.23818812E−03	0	0	This work
$\Psi_{K,Sr,Cl}$ (273.15–298.15 K)	2.53166696E−02	−1.67691997E−04	0	0	This work
$\Psi_{K,Sr,Cl}$ (298.15–323.15 K)	−2.12423724E−01	5.93075752E−04	0	0	This work
$\Psi_{K,Sr,Cl}$ (323.25–373.15 K)	−1.57500682E−01	4.44695765E−04	0	0	This work
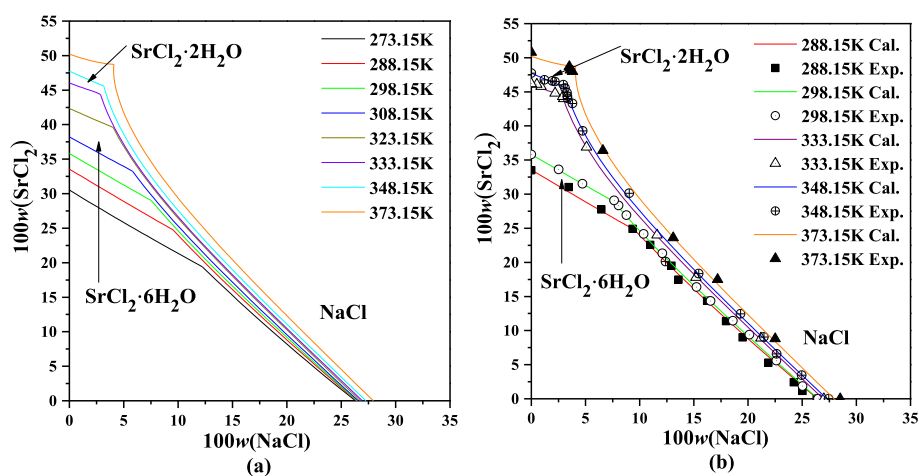
Fig. 1. Calculated and experimental phase diagrams of the ternary system NaCl–SrCl$_2$–H$_2$O at different temperatures. (a) Solid lines, calculated data. (b) solid lines, calculated data; symbols, experimental data; ■, 288.15 K, from Ref. [15]; ○, 298.15 K, from Ref. [12]; △, 333.15 K, from Ref. [11]; ⊕, 348.15 K, in Ref. [14]; ▲, 373.15 K, in Ref. [11].
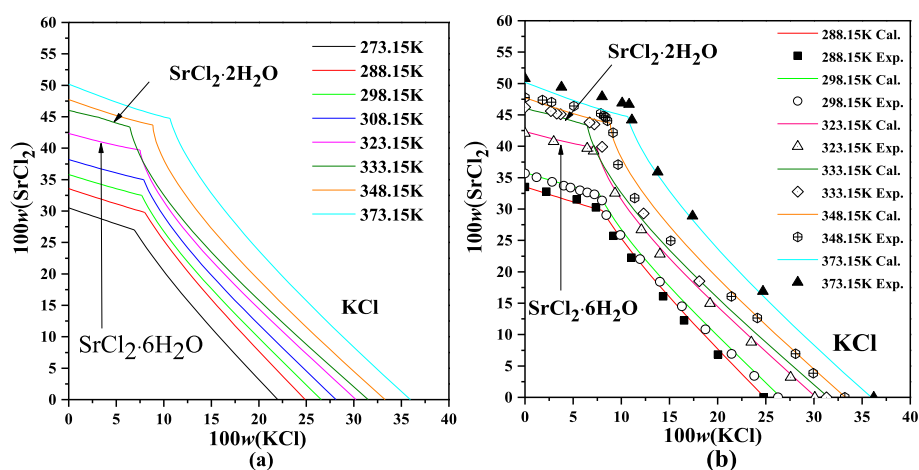
Fig. 2. Calculated and experimental phase diagrams of the ternary system KCl–SrCl$_2$–H$_2$O at different temperatures. (a) Solid lines, calculated data. (b) solid lines, calculated data; symbols, experimental data; ■, 288.15 K, from Ref. [18]; ○, 298.15 K, from Ref. [13]; △, 323.15 K, from Ref. [16]; ◇, 333.15 K, from Ref. [11]; ⊕, 348.15 K, in Ref. [14]; ▲, 373.15 K, in Ref. [11].
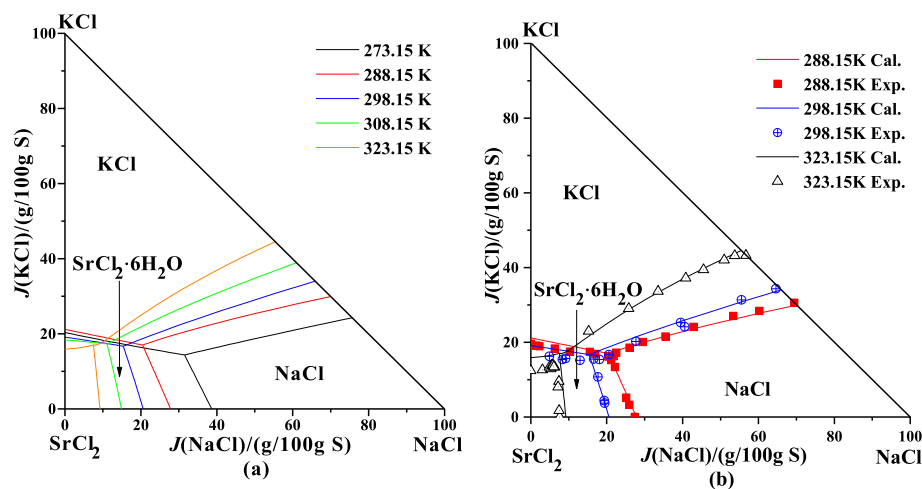
Fig. 3. Calculated and experimental phase diagrams of the quaternary system NaCl–KCl–SrCl$_2$–H$_2$O at different temperatures. Solid lines, calculated data; symbols, experimental data. (a) Solid lines, calculated data. (b) Solid lines, calculated data; symbols, experimental data; ■, 288.15 K, from Ref. [18]; ⊕, 298.15 K, from Ref. [12]; △, 323.15 K, from Ref. [16].

Table 2
The calculated osmotic coefficients, water activity and ionic activity coefficients of the quaternary system NaCl–KCl–SrCl$_2$–H$_2$O at 273.15 K.

No.	Composition of the liquid phase mol/kg H$_2$O				Osmotic coefficients	Water activity	Ionic activity coefficients				Equilibrium solid phase
	Na$^+$	K$^+$	Sr^{2+}	Cl$^-$	ϕ	a_w	γ-Na	γ-K	γ-Sr	γ-Cl	
1	5.4632	1.3736	0.0000	6.8367	1.2390	0.7370	0.9676	0.4845	–	0.8774	NaCl + KCl
2	5.1145	1.3233	0.2000	6.8378	1.2735	0.7341	0.9406	0.4577	0.6768	0.9639	NaCl + KCl
3	4.7770	1.2749	0.4000	6.8519	1.3095	0.7306	0.9170	0.4326	0.6844	1.0564	NaCl + KCl
4	4.4503	1.2283	0.6000	6.8786	1.3470	0.7267	0.8969	0.4092	0.6968	1.1548	NaCl + KCl
5	4.1341	1.1834	0.8000	6.9175	1.3862	0.7222	0.8803	0.3872	0.7141	1.2595	NaCl + KCl
6	3.8283	1.1401	1.0000	6.9684	1.4272	0.7171	0.8671	0.3666	0.7364	1.3708	NaCl + KCl
7	3.5326	1.0985	1.2000	7.0311	1.4698	0.7114	0.8574	0.3472	0.7642	1.4888	NaCl + KCl
8	3.2473	1.0583	1.4000	7.1056	1.5142	0.7051	0.8514	0.3289	0.7979	1.6141	NaCl + KCl
9	2.9722	1.0196	1.6000	7.1919	1.5603	0.6981	0.8491	0.3116	0.8384	1.7469	NaCl + KCl
10	3.0613	0.0000	1.7914	6.6441	1.6668	0.7081	0.7678	–	0.7475	2.0304	NaCl + SrCl$_2$·6H$_2$O
11	3.0316	0.1000	1.7871	6.7058	1.6592	0.7065	0.7758	0.2906	0.7603	2.0105	NaCl + SrCl$_2$·6H$_2$O
12	3.0018	0.2000	1.7829	6.7677	1.6516	0.7049	0.7839	0.2915	0.7731	1.9910	NaCl + SrCl$_2$·6H$_2$O
13	2.9721	0.3000	1.7789	6.8299	1.6443	0.7033	0.7920	0.2925	0.7860	1.9723	NaCl + SrCl$_2$·6H$_2$O
14	2.9424	0.4000	1.775	6.8923	1.6371	0.7017	0.8002	0.2934	0.7988	1.9539	NaCl + SrCl$_2$·6H$_2$O
15	2.9127	0.5000	1.7712	6.9550	1.6300	0.7002	0.8084	0.2943	0.8117	1.9361	NaCl + SrCl$_2$·6H$_2$O
16	2.8830	0.6000	1.7675	7.0180	1.6230	0.6986	0.8168	0.2953	0.8246	1.9186	NaCl + SrCl$_2$·6H$_2$O
17	2.8534	0.7000	1.7639	7.0812	1.6162	0.6970	0.8252	0.2962	0.8374	1.9017	NaCl + SrCl$_2$·6H$_2$O
18	2.8237	0.8000	1.7605	7.1447	1.6095	0.6954	0.8337	0.2972	0.8502	1.8852	NaCl + SrCl$_2$·6H$_2$O
19	0.0000	1.4014	2.5787	6.5587	1.5164	0.7498	–	0.2479	0.5071	1.7524	KCl + SrCl$_2$·6H$_2$O
20	0.3000	1.3474	2.4846	6.6166	1.5262	0.7441	0.6518	0.2531	0.5313	1.7690	KCl + SrCl$_2$·6H$_2$O
21	0.6000	1.2961	2.3917	6.6795	1.5356	0.7383	0.6718	0.2585	0.5582	1.7840	KCl + SrCl$_2$·6H$_2$O
22	0.9000	1.2473	2.3000	6.7473	1.5447	0.7323	0.6929	0.2639	0.5883	1.7976	KCl + SrCl$_2$·6H$_2$O
23	1.2000	1.2008	2.2095	6.8197	1.5535	0.7262	0.7152	0.2694	0.6218	1.8099	KCl + SrCl$_2$·6H$_2$O
24	1.5000	1.1565	2.1201	6.8966	1.5622	0.7200	0.7385	0.2749	0.6593	1.8209	KCl + SrCl$_2$·6H$_2$O
25	1.8000	1.1143	2.0317	6.9777	1.5706	0.7136	0.7630	0.2805	0.7013	1.8306	KCl + SrCl$_2$·6H$_2$O
26	2.1000	1.0740	1.9445	7.0630	1.5790	0.7072	0.7887	0.2862	0.7483	1.8392	KCl + SrCl$_2$·6H$_2$O
27	2.7672	0.9907	1.7543	7.2665	1.5970	0.6924	0.8501	0.2990	0.8746	1.8550	NaCl + KCl + SrCl$_2$·6H$_2$O

co-saturated point of the quaternary system and decreases with increasing temperature in Fig. 4. From Fig. 5, the activity coefficients for Sr^{2+} has maximum values at co-saturated point of the quaternary system and increase with increasing temperature, which shows a opposite trends with that in Fig. 4.

5. Chemical engineering process simulation

5.1. Isothermal evaporation calculation at 298.15 K

The Pitzer model for the system NaCl–KCl–SrCl$_2$–H$_2$O at 298.15 K was applied for the isothermal evaporation calculation, which was described in our previous wok [24]. The original compo-

sition of the ions used in the calculation was cited from literature [1], as shown in Table 3. It is assumed that there are only sodium chloride, potassium chloride and strontium chloride in the brine of the solar pond for convenience. The calculated phase diagram of the system NaCl–KCl–SrCl$_2$–H$_2$O at 298.15 K was used to explain the evolution evaporation process. The evaporation-crystallization path of the brine was plotted, as shown in Fig. 6.

Point A shows the original brine, which is unsaturated solution for all the salts, located in the KCl crystallization region in the dry-salt diagrams in Fig. 6. From point A to point B, the brine is concentrated continuously, but no salt is precipitated out from the brine. The liquid phase then gets into the area saturated with KCl, with KCl precipitating out from the brine at point B. As KCl continues precipitating out from the brine, the evaporation-crystallization
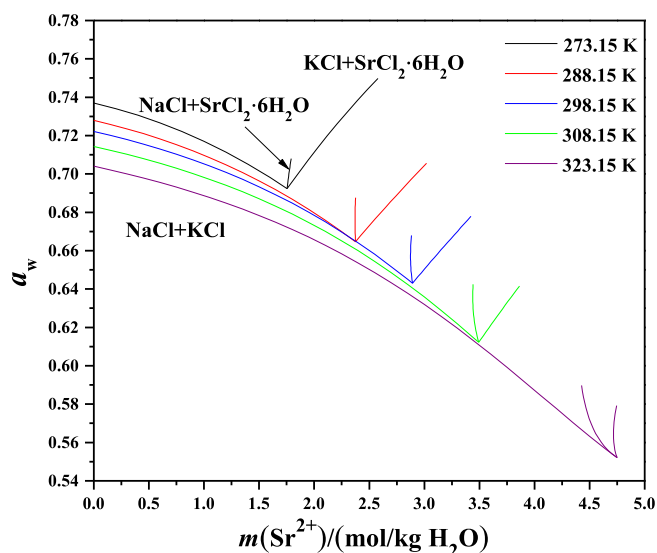
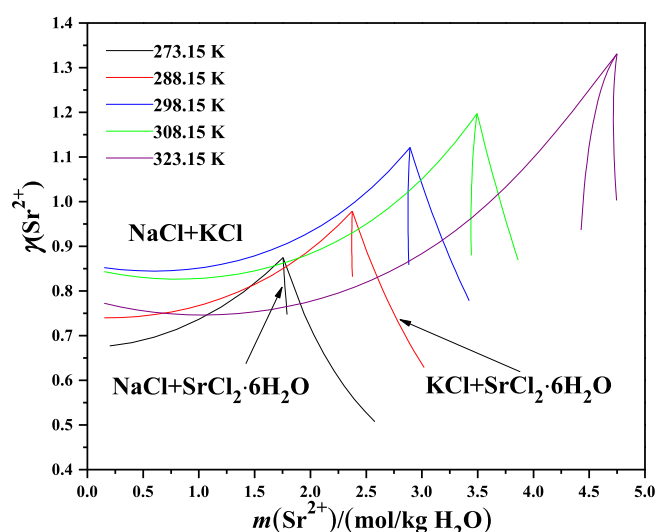Fig. 4. Calculated water activity a_w of the quaternary system NaCl–KCl–SrCl$_2$–H$_2$O from 273.15 K to 323.15 K.
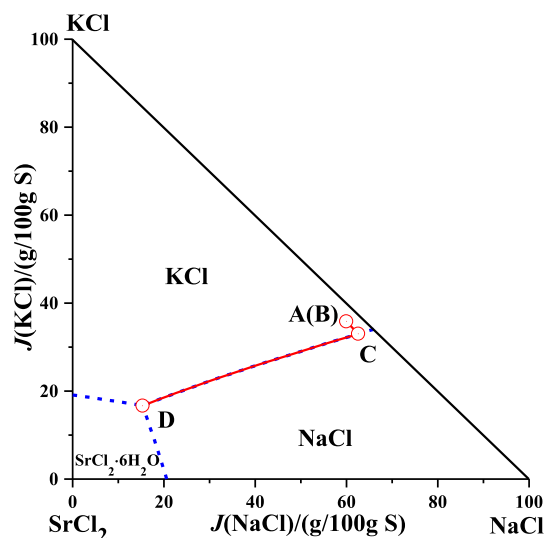

Fig. 6. Evaporation–crystallization route with the phase diagram of NaCl–KCl–SrCl$_2$–H$_2$O system at 298.15 K. ○, solid phase points; —, brine separation route; ⋯, solubility curves.

Fig. 5. Calculated Sr^{2+} activity coefficients γ of the quaternary system NaCl–KCl–SrCl$_2$–H$_2$O at different temperatures.

path follows the line from the point of pure KCl to point B, then to point C in Fig. 6. From B to C, the evaporation ratio is only from 51.92% to 54.96%, and pure KCl obtained is only 11.73% for total KCl. Sodium chloride is saturated at point C with KCl and NaCl precipitating out as evaporation goes on. The evaporation-crystallization path follows the curve cosaturated with KCl and NaCl to the invariant point D. Then, SrCl$_2$·6H$_2$O will precipitate out from the liquid phase at point D, accompanied by the precipitation of KCl and NaCl. When SrCl$_2$·6H$_2$O begins to precipitate out, the evaporation ratio is 97.95%. About 98.38% of NaCl and 97.03% of KCl are precipitated out from the brine. The composition of the liquid phase at point D becomes stable till the brine is dried.

As shown in Fig.6, the brine separation process can be separated into four stages: water evaporation stage (AB), KCl crystallization stage (BC), NaCl crystallization stage (CD), and SrCl$_2$·6H$_2$O crystallization stage. The salts precipitate out from the brine are in order of KCl, NaCl, and SrCl$_2$·6H$_2$O. Only pure KCl can be obtained from the evaporation process with these steps.

5.2. Brine separation with Pitzer model at 273.15 K and 323.15 K

The phase diagrams of brine systems at various temperatures were always used in the chemical engineering process of brines because the brine temperature is changing all the time. The aver-

Table 3
Chemical composition of the liquid phases during brine separation for system NaCl–KCl–SrCl$_2$–H$_2$O at 273.15 K and 323.15 K.

| No.	Evaporation ratio/%[a]	Chemical components of the liquid phase/(mol·kg^{-1})			Salt precipitation
		NaCl	KCl	SrCl$_2$	
A	0.00	2.2738	1.0659	0.0592	none
B	54.55	5.0023	2.3451	0.1303	none
C	64.92	4.6619	3.0379	0.1687	NaCl
D	67.81	5.0815	1.3089	0.1839	KCl
E	85.82	4.3985	2.9713	0.4175	NaCl
F	86.50	4.6185	1.2620	0.4384	KCl
G	93.94	3.8220	2.8142	0.9776	NaCl
H	93.94	3.8220	1.1313	0.9776	KCl
I	97.25	2.7211	2.4889	2.1507	NaCl
J	96.80	2.3401	1.0425	1.8496	KCl
K	98.43	1.6145	2.1266	3.7732	NaCl
L	98.75	1.2902	2.2896	4.7496	NaCl + KCl
M	97.49	0.7199	12,776	2.3546	SrCl$_2$·6H$_2$O
N	98.67	1.3607	2.1674	4.4501	KCl
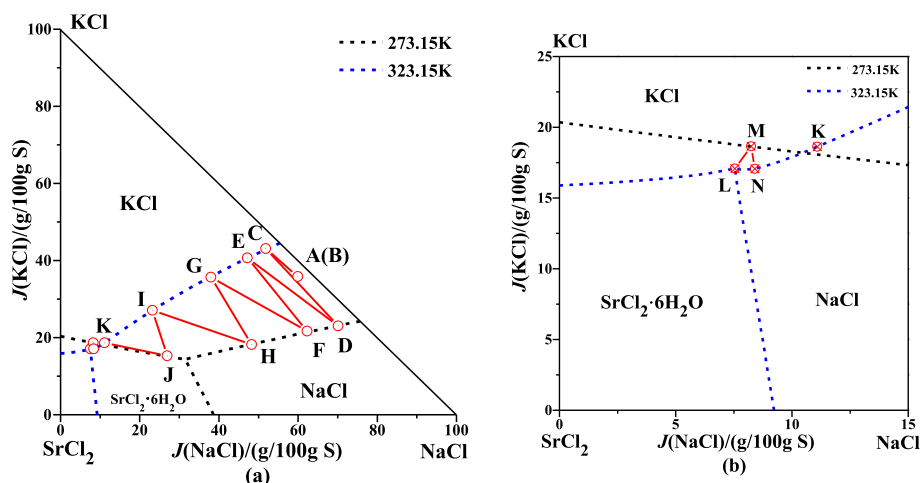
Fig. 7. Brine separation route with the phase diagrams of system NaCl–KCl–SrCl$_2$–H$_2$O at 273.15 K and 323.15. —, brine separation route; ..., solubility curves.

age temperature of the brine is about 273.15 K, while the temperature for the brine in the solar ponds in summer can reach up to 323.15 K. Thus, the phase diagrams in system NaCl–KCl–SrCl$_2$–H$_2$O calculated with Pitzer model at 273.15 and 323.15 K in Fig. 7 were used in the simulated separation process of strontium chloride from solution. The flow chart for the separation process was shown in Fig. 8.

The point A in Fig. 7 is in KCl crystallization zone at 273.15 K, while in NaCl crystallization zone at 323.15 K. The evaporation at 323.15 K was firstly applied because of its high evaporation speed at high temperature. The process from point A to point B is the water evaporation stage without NaCl precipitating out from the solution. BC is the process of NaCl crystallization stage at 323.15 K. KCl begins to saturate at point C, which is in the KCl crystallization zone of the phase diagram at 273.15 K. Therefore, the evaporation stopped at point C when the solution is saturated with KCl. The solution and solid phase NaCl were separated.

The solution at 323.15 K was then cooled down to 273.15 K. From the Pitzer model, KCl will precipitate out from the solution in cooling down process. CD is the process for KCl crystallization stage at 273.15 K. At point D, the evaporation stopped to separate solid phase KCl. And then, the solution was heated to 323.15 K to get solid phase NaCl with evaporation method. These steps were repeated to get pure NaCl and KCl till to the point K. The process from I to J is different from the other stage. The solution at point I was firstly diluted and then cooled down to prevent NaCl crystallization. The point K is in the KCl crystallization zone at 273.15 K, but it's very close to the curve saturated with KCl and NaCl. Therefore, only small KCl can be obtained if the solution evaporated at 273.15 K. Therefore, the solution at point K was still evaporated at 323.15 K with both NaCl and KCl crystallization.

The evaporation stopped at point L when the solution was saturated with SrCl$_2$·6H$_2$O. The point L, which is the invariant point of the phase diagram in system NaCl–KCl–SrCl$_2$–H$_2$O at 323.15 K, is in the SrCl$_2$·6H$_2$O crystallization zone at 273.15 K. The solution at point L was firstly diluted and then cooled down to 273.15 K. The pure SrCl$_2$·6H$_2$O was precipitated out form the solution in the cooling process. The evaporation-crystallization path then follows the line from the point of SrCl$_2$ to point L. The evaporation is stopped at point M to get the maximum SrCl$_2$·6H$_2$O. And then, the solution is heated to 323.15 K and evaporated to obtain KCl to the point N. Point N is in the curve saturated with NaCl and KCl at 323.15 K. From N to L, the mixture of NaCl and KCl was obtained with evaporation continuously at 323.15 K. The steps were repeated to get pure SrCl$_2$·6H$_2$O continuously. All SrCl$_2$·6H$_2$O can be obtained with the above method theoretically.
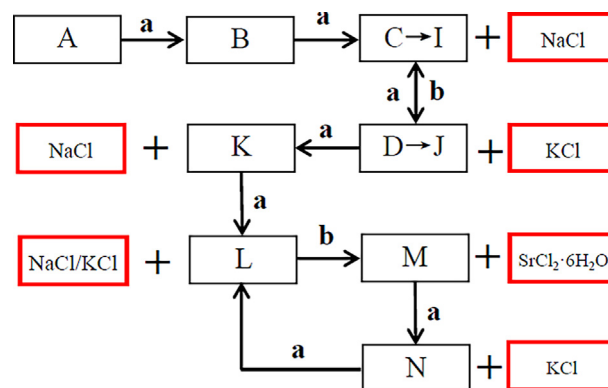

Fig. 8. The flow chart for the brine separation process with the phase diagrams of NaCl–KCl–SrCl$_2$–H$_2$O system at 273.15 K and 323.15 K. a, evaporation at 323.15 K; b, cooling down to 273.15 K and evaporation at 273.15 K.

The calculated compositions of the solution in molality for these points are tabulated in Table 3. The unit of molality (mol·kg^{-1}) was used in the modeling calculations, so the amount of brine containing 1 kg water was used for convenience. From Table 3, about 98.89% of NaCl and more than 96.87% of KCl can be separated from the solution. From these steps, sodium chloride, potassium chloride and strontium chloride were separated. Pure NaCl, KCl and SrCl$_2$·6H$_2$O were obtained from the solution with evaporation method at 273.15 K and 323.15 K. The process with the phase diagrams at 273.15 K and 323.15 K is better than that only with the phase diagram at 298.15 K. The results for the real brine are not always consistent with the solubility curves in phase diagram because the brine system is more complicated than this quinary system. However, the phase diagram can still supply the theoretical foundation for exploitation of brine resources.

6. Conclusions

Combining the experimental solubilities of two ternary systems NaCl–SrCl$_2$–H$_2$O and KCl–SrCl$_2$–H$_2$O, and Pitzer binary parameters obtained in the literatures at different temperatures, the lacking Pitzer mixing parameters $\theta_{\mathrm{Na,Sr}}$, $\theta_{\mathrm{K,Sr}}$, $\Psi_{\mathrm{Na,Sr,Cl}}$, and $\Psi_{\mathrm{K,Sr,Cl}}$ were fitted on the basis of the Pitzer model. The temperature dependence of the interaction parameters including Sr^{2+} ion was built. The model was then used to calculate the solubilities, water activities and ionic activity coefficients of the quaternary system NaCl–

KCl–SrCl$_2$–H$_2$O in the wider temperature range. The theoretical solubilities using the model coincide with the experimental values. The phase diagrams and Pitzer model for the quaternary system were then used to conduct computer simulation of isothermal evaporation and brine separation. The evaporation-crystallization route and the order of salt crystallization were demonstrated using the diagram of the quaternary system at 298.15 K. The minerals were crystallized out of the brine in the order of KCl, NaCl and SrCl$_2$·6H$_2$O, and the entire evaporation process may consist of four stages. The brine separation process route was demonstrated at 273.15 K and 323.15 K. The salts KCl, NaCl and SrCl$_2$·6H$_2$O were separated from the solution with the model at 273.15 K and 323.15 K. This simulation results can supply fundamental data for salt separation and purification of brine systems.

Acknowledgments

References

[1] Q.S. Fan, H.Z. Ma, H.B. Tan, T.W. Li, Hydrochemical anomaly and resources evaluation of the oil fields brines in the typical area of western Qaidam Basin (in Chinese), J. Salt Lake Res. 15 (2007) 6–12.

[2] P.S. Song, The phase diagram of salt-water systems and utilization of Salt Lake resources (in Chinese), J. Salt Lake Res. 24 (2016) 35–49.

[3] M. Zheng, Y. Zhang, X. Liu, W. Qi, F. Kong, Z. Nie, L. Pu, X. Hou, H. Wang, Z. Zhang, W. Kong, Y. Lin, Progress and prospects of Salt Lake Research in China, Acta Geol. Sin. (Engl. Ed.) 90 (2016) 1195–1235.

[4] K.S. Pitzer, Thermodynamics of electrolytes. I. Theoretical basis and general equations, J. Phys. Chem. 77 (1973) 268–277.

[5] K.S. Pitzer, Ion interaction approach: theory and data correlation, in: Activity Coefficients in Electrolyte Solutions, 2nd ed., CRC Press, Boca Raton, FL, 1991, pp. 75–153, Chapter 3.

[6] C.E. Harvie, J.H. Weare, The prediction of mineral solubilities in natural waters: the Na–K–Mg–Ca–Cl–SO$_4$–H$_2$O system from zero to high concentration at 25 °C, Geochim. Cosmochim. Acta 44 (1980) 981–997.

[7] C.E. Harvie, H.P. Eugster, J.H. Weare, Mineral equilibria in the six-component seawater system, Na–K–Mg–Ca–SO$_4$–Cl–H$_2$O at 25 °C. II: Compositions of the saturated solutions, Geochim. Cosmochim. Acta 46 (1982) 1603–1618.

[8] C.E. Harvie, N. Møller, J.H. Weare, The prediction of mineral solubilities in natural waters: the Na-K-Mg-Ca-H-Cl-SO$_4$-OH-HCO$_3$-CO$_3$-CO$_2$-H$_2$O system to high ionic strengths at 25 °C, Geochim. Cosmochim. Acta 48 (1984) 723–751.

[9] A.R. Felmy, J.H. Weare, The prediction of borate mineral equilibria in natural waters: application to Searles Lake, California, Geochim. Cosmochim. Acta 50 (1986) 277–2783.

[10] C.E. Harvie, J.P. Greenberg, J.H. Weare, A chemical equilibrium algorithm for highly non-ideal multiphase systems: free energy minimization, Geochim. Cosmochim. Acta 51 (1987) 1045–1057.

[11] G.O. Assarsson, Equilibria in aqueous systems containing Sr^{2+}, K$^+$, Na$^+$, and Cl$^-$, J. Phys. Chem. 57 (1953) 207–210.

[12] V.K. Filippov, Y.A. Fedorov, N.A. Charykov, Thermodynamics of phase equilibria in the potassium, strontium, sodium, chloride, water (K$^+$, Sr^{2+}/Cl$^-$–H$_2$O, Na$^+$, Sr^{2+}/Cl$^-$–H$_2$O and Na$^+$, K$^+$, Sr^{2+}/Cl$^-$–H$_2$O) system at 25 °C, Zh. Obshch. Khim. 60 (1990) 492–499.

[13] L.J. Shi, B. Sun, X.P. Ding, P.S. Song, Phase equilibria in ternary system KCl–SrCl$_2$–H$_2$O at 25 °C (in Chinese), Chin. J. Inorg. Chem. 26 (2010) 333–338.

[14] D.W. Li, S.H. Sang, R.Z. Cui, C. Wei, Solid–liquid equilibria in the ternary systems NaCl–SrCl$_2$–H$_2$O and KCl–SrCl$_2$–H$_2$O at 348 K, J. Chem. Eng. Data 60 (2015) 1227–1232.

[15] D. Li, Q.F. Meng, L.Z. Meng, X.X. Fan, Solid−liquid equilibria in the NaCl–SrCl$_2$–H$_2$O system at 288.15 K, Russ. J. Phys. Chem. A 90 (2016) 368–373.

[16] X. Zhang, S.H. Sang, S.Y. Zhong, W.Y. Huang, Equilibria in the ternary system SrCl$_2$–KCl–H$_2$O and the quaternary system SrCl$_2$–KCl–NaCl–H$_2$O at 323 K, Russ. J. Phys. Chem. A 89 (2015) 2322–2326.

[17] H.J. Han, L.J. Guo, D.D. Li, Y. Yao, Water activity and phase equilibria measurements and model simulation for the KCl–SrCl$_2$–H$_2$O system at 323.15 K, J. Chem. Eng. Data 62 (2017) 3753–3757.

[18] L.Z. Meng, X. Wang, D. Li, T.L. Deng, Y.F. Guo, L. Yang, Experimental determination and thermodynamic modeling of solid–liquid equilibria in the quaternary system NaCl–KCl–SrCl$_2$–H$_2$O at 288.15 K, J. Chem. Eng. Data 63 (2018) 4410–4417.

[19] D.C. Reddy, J. Ananthaswamy, Thermodynamic properties of aqueous electrolyte solutions: an e.m.f. study of {KCl(m_A) + SrCl$_2$(m_B)}(aq) at the temperatures 298.15 K, 308.15 K, and 318.15K, J. Chem. Thermodyn. 22 (1990) 1015–1023.

[20] M.F. Zhou, S.H. Sang, Q.Z. Liu, D. Wang, C. Fu, Mean activity coefficients of NaCl in NaCl + SrCl$_2$ + H$_2$O ternary system at 298.15 K determined by potential difference measurements, J. Chem. Eng. Data 60 (2015) 3209–3214.

[21] S.L. Clegg, Isopiestic determination of the osmotic and activity coefficients of NaCl + SrCl$_2$ + H$_2$O at 298.15 K and representation with an extended ion-interaction model, J. Chem. Eng. Data 50 (2005) 1162–1170.

[22] J.P. Greenberg, N. Møller, The prediction of mineral solubilities in natural waters: a chemical equilibrium model for the Na-K-Ca-Cl-SO$_4$-H$_2$O system to high concentration from 0 to 250 °C, Geochim. Cosmochim. Acta 53 (1989) 2503–2518.

[23] M. Steiger, Thermodynamic properties of SrCl$_2$(aq) from 252 K to 524 K and phase equilibria in the SrCl$_2$–H$_2$O system: Implications for thermochemical heat storage, J. Chem. Thermodyn. 120 (2018) 106–115.

[24] L.Z. Meng, M.S. Gruszkiewicz, T.L. Deng, Y.F. Guo, D. Li, Isothermal evaporation process simulation using Pitzer model for the quinary system LiCl–NaCl–KCl–SrCl$_2$–H$_2$O at 298.15 K, Ind. Eng. Chem. Res. 54 (2015) 8311–8318.

JCT 19-9